Applied Mathematical Modelling 37 (2013) 6244–6253

Contents lists available at SciVerse ScienceDirect

Applied Mathematical Modelling

journal homepage: www.elsevier.com/locate/apm

Battery state-of-charge estimator using the SVM technique

J.C. Álvarez Antón [a,*], P.J. García Nieto [b], F.J. de Cos Juez [c], F. Sánchez Lasheras [d], M. González Vega [a], M.N. Roqueñí Gutiérrez [c]

[a] Department of Electrical Engineering, Campus de Viesques, University of Oviedo, 33204 Gijón, Spain
[b] Department of Mathematics, Faculty of Sciences, University of Oviedo, 33007 Oviedo, Spain
[c] Mining Exploitation and Prospecting Department, University of Oviedo, 33004 Oviedo, Spain
[d] Department of Construction and Manufacturing Engineering, University of Oviedo, 33204 Gijón, Spain

ARTICLE INFO

Article history:
Received 31 July 2012
Received in revised form 10 November 2012
Accepted 10 January 2013
Available online 20 January 2013

Keywords:
Lithium batteries
Modeling
State-of-charge (SOC)
Support vector machine (SVM)
Support vector regression

ABSTRACT

State-of-charge (SOC) is the equivalent of a fuel gauge for a battery pack in an electric vehicle. Determining the state-of-charge becomes an important issue in all battery applications including electric vehicles (EV), hybrid electric vehicles (HEV) or portable devices. The aim of this innovative study is to estimate the SOC of a high capacity lithium iron phosphate ($LiFePO_4$) battery cell from an experimental data-set obtained in the University of Oviedo Battery Laboratory (UOB Lab) using support vector machine (SVM) approach. The SOC of a battery cannot be measured directly and must be estimated from measurable battery parameters such as current, voltage or temperature. An accurate predictive model able to forecast the SOC in the short term is obtained. The agreement of the SVM model with the experimental data-set confirmed its good performance.

1. Introduction

One of the most important battery parameters is the battery state-of-charge (SOC). Knowing the amount of energy left in a battery compared with the energy it had when it was full, gives the user an indication of how much longer a battery will continue to perform before it needs recharging. Using the analogy of a fuel tank in a car, State of charge (SOC) estimation is often called the "Gas Gauge" or "Fuel Gauge" function. The SOC is defined as the available battery capacity expressed as a percentage of its rated capacity, where 100% implies a full battery state and 0% the empty state. The battery capacity is usually measure in Ampere-hour (Ah). Determining and controlling the SOC is critically important in multiple applications. These applications require accurate measurement of battery SOC in order to give users an indication of available runtime. SOC estimation can also be useful to avoid detrimental situations, such as over-discharging and over-charging, which can lead to a reduction in battery life. Accurate SOC indication is thus important for user convenience and for prolonging the lifetime of batteries. However, many examples of poor accuracy and reliability are found in practice. The main problem of designing an accurate SOC indication system is the unpredictability of both battery and user behavior.

Several techniques have been reported for measuring or estimating the SOC of battery cells [1]. The most common methods include current integration techniques, artificial neural networks and fuzzy logic based estimations [2], Kalman filter-based estimators [3–5] and others [6–9]. Most of these methods have been widely used and achieve acceptable results in different applications. The most common technique for calculating SOC is the ampere-hour counting. The method is based on current measurement and integration during the charge and discharge state. One drawback of current integration

* Corresponding author. Address: University of Oviedo, Department of Electrical Engineering, Campus de Viesques, Campus de Viesques, Modulo 3. Room 3-2-13, 33204 Gijón, Spain. Tel.: +34 985182553; fax: +34 985182138.
E-mail address: anton@uniovi.es (J.C. Álvarez Antón).

0307-904X/$ - see front matter © 2013 Elsevier Inc. All rights reserved.
http://dx.doi.org/10.1016/j.apm.2013.01.024

techniques is their reduced accuracy. Other methods exhibit greater performance, but a high implementation cost is required due to their computational complexity.

SVM techniques (SVMs) [10–12] have developed greatly in recent years, giving rise to a new kind of learning machines that use the central concept of SVMs, namely, kernels, for a number of learning tasks. Kernel machines provide a modular framework that can be adapted to different tasks and domains by using different kernel function (i.e., linear, polynomial, sigmoid or radial basis) and the base algorithm [13]. They are used in a variety of fields, including biomedicine and bioinformatics [14], image analysis and artificial vision [15] and other engineering fields [16,17]. Like conventional feedforward neural networks such as the multilayer perceptron (MLP) [18], SVMs have been used by researchers to solve classification and regression problems [19]. Several research studies demonstrate the good performance of these techniques in the battery modeling [20]. In this research study, SVM for regression (SVR) is used as automated learning tool with a different focus to successfully predict the SOC of a high capacity lithium iron phosphate ($LiFePO_4$) battery cell as a function of cell voltage, cell current and cell temperature. SVM model is used as an alternative to the traditional regression approaches. The SVM used as a nonlinear estimator is more robust than a least-squares estimator because it is insensitive to small changes.

2. Materials and methods

2.1. Experimental battery cell and test workbench

Lithium-ion is the newest battery chemistry and is now well understood and widely used in numerous applications thanks to its high cell voltage, high energy density, long lifetime and exceptional cyclability. A $LiFePO_4$ battery cell with a nominal capacity of 100 A h is used in this study. The main cell characteristics are summarized in Table 1.

The battery-testing platform consists of programmable stand-alone instruments and a computer-control unit using National Instrument LabVIEW™ software [21]. The test workbench block diagram is shown in Fig. 1. Stand-alone instruments are modular/independent instruments that support a wide variety of functions in the power and measurement field. In this case, a programmable power source (Sorensen DHP series, 60-220 M1-M9D, 0–60 V, 0–220 A) is used for cell charging. An electronic load (Agilent 6050A with three 60504B modules) is used for discharging purpose. Battery voltage, temperature and other variables used for charging sensing termination [22] are monitored using a modular data acquisition system (Agilent 34970A) with a total accuracy of 260 μV for dc measures. Battery cell temperature is measured using a resistance temperature detector (RTD) attached to the centre of the module. RTDs are temperature sensors that contain a resistor that changes the resistance value as its temperature changes. Internal power source and electronic load meters are used to provide current measurements with an accuracy of 0.12% ± 130 mA. All data measurements are taken at a sample rate of 5 s. Battery performance largely depends on temperature, so all tests commence at the initial temperature of 23 ± 2 °C in an electronically controlled environmental chamber. The workbench is controlled by a custom software application written in the National Instrument LabVIEW™ software. A description of the workbench and operating details can be found in [23].

2.2. Experimental data set

The most reliable test for determining the SOC of a battery is a discharge test at a particular C-rate under controlled conditions. This test includes a consecutive battery recharge. Charging and discharging currents are generally expressed as multiples of C, where C is the battery nominal capacity. C-rate is a value which expresses the rated current capacity of a cell or battery. For example, a cell discharging at the C-rate will deliver its nominal rated capacity for 1 h. The time to discharge a battery is inversely proportional to the discharge rate. Multiples larger or smaller than the C-rate are used to express larger or smaller currents. For example, the C-rate is 100 A in the case of a 100 A h battery, while the C/2 and 2C-rates are 50 A and 200 A, respectively. In this paper, three consecutive cycles of charging and discharging at different C-rates are performed using a CALB $LiFePO_4$ battery cell with a nominal capacity of 100 A h. Cell variables (voltage, current and temperature)

Table 1
High capacity lithium iron phosphate ($LiFePO_4$) battery cell characteristics.

Parameter	Value
Manufacturer	CALB
Model	SE100AHA
Nominal capacity	100 A h
Nominal voltage	3.2 V
Energy density	105 w h/kg at 0.1C
Charging/discharging cut-off voltage	3.6 V/2.5 V
Recommend charging current	0.3 C 30 A
Maximum discharge current (short-tine < 10 s)	800 A
Cycle life (at 80% DoD, 0.3 C)	2000 times
Operating temperature (charge/discharge)	0 °C–45 °C/−20 °C–55 °C
Shell material	Plastic
Weight	3.2 kg

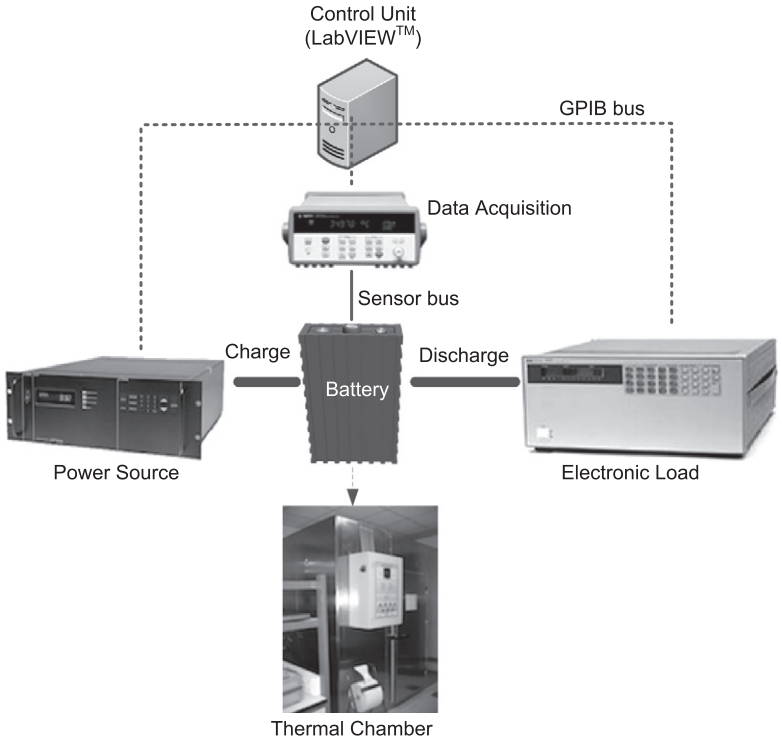

Fig. 1. Test battery workbench architecture.

are measured during charging and discharging to identify the model parameters. Experimental data are obtained in two steps using the workbench described previously. During the first step the battery is fully charged using the usual Constant-Current-Constant-Voltage (CCCV) charging method at a 0.3 C-rate charging current until reaching 3.6 V. Full charge occurs when the battery reaches the voltage threshold of 3.6 V and the current drops to five percent of the rated current. Manufacturers of Li-ion cells are very strict on the correct setting of this maximum voltage because Li-ion cannot accept overcharge. A cell voltage greater than 3.6 V causes stress and reduces the battery life. In the CV mode the voltage is then kept constant at 3.6 V while the charging process continues in constant voltage mode until the charge current has dropped to 0.05C. The full SOC (100%) is reached in this situation. Second, after a rest period, the battery is discharged at constant current until reaching the cut-off voltage of 2.5 V. This process is repeated three times at different discharging rates, as shown in Figs. 2–4.

The main goal of this research work is to obtain a model to estimate the SOC using the SVM technique. Figs. 2 and 3 show the temperature, current, voltage and SOC ranges of the training data for the SVM model. Fig. 4 shows the data-set used to validate the SVM model. The main difference between the data collection reported in Figs. 2–4 is the load that is used for battery discharge. The current used for battery discharge is fixed at C (-100 A) in Fig. 2, at C/3 (-33 A) in Fig. 3 and at C/2 (-50 A) in Fig. 4. The model training data covers operating from 100% SOC to 0% SOC and back up to 100% SOC. All data points in this SOC range are used for training. The training current goes from 30 A to -100 A and 30 A to -33 A; see Figs. 2 and 3 respectively. Validation data covers the same SOC range, but current goes from 30 A to -50 A. Additionally, several plateaus with 0 A current and steady-state SOC are also included as training and validation data. These plateaus correspond to phases of the battery rest time. Rest period is always used to stabilize chemical reactions inside the battery. The model also uses the data supplied during the rest time in order to predict the battery behavior in that period.

2.3. Support vector machine method (SVM)

SVMs are a set of related supervised learning methods used for classification and regression that can universal approximate any multivariate function to any level of accuracy [11]. SVMs were originally developed to solve classification problems. They were later generalized to solve regression problems [24,10] in a method called support vector regression (SVR). The model produced by support vector classification only depends on a subset of the training data, because the cost function for building the model ignores training points that lie beyond the margin. Analogously, the model produced by SVR only depends on a subset of the training data, because the cost function for building the model ignores any training data that are close (within a threshold ε) to the model prediction.

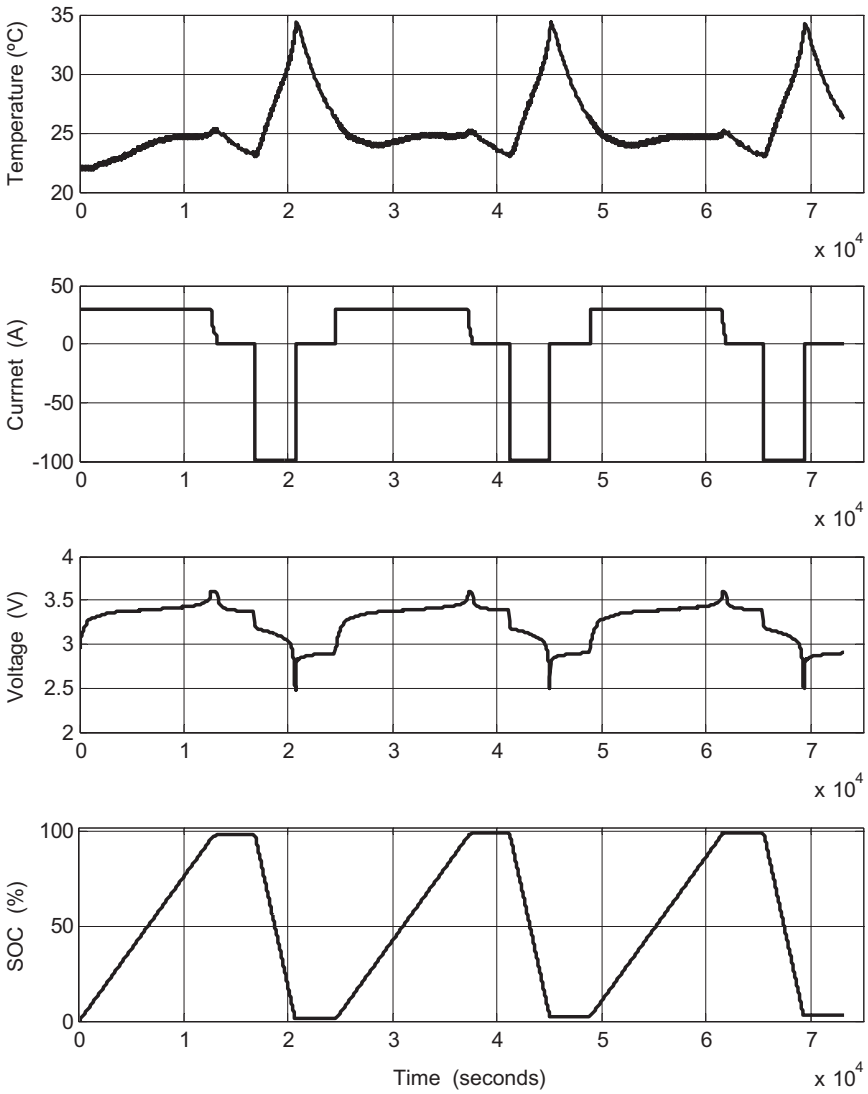

Fig. 2. Training data: cell temperature, current, voltage and SOC vs. time during three charging–discharging cycles. Discharge current is set at C rate (100A).

The basic idea of SVR is briefly described here. Rather than classify new unseen variables $\hat{\vec{x}}$ into one of two categories $\hat{y} = \pm 1$, we want to predict a real-valued output for $y^{'}$. Hence, the training data is of the form $\{\vec{x}_i, t_i\}$, where $i = 1, 2, \ldots, L, y_i, \in \Re$, $\vec{x} \in \Re^D$ [24,19]:

$$y_i = \vec{w} \cdot \psi(\vec{x}_i) + b, \tag{1}$$

where $\vec{w}$ controls the smoothness of the model, $\psi(\vec{x}_i)$ is a function of projection of the input space to the feature space, b is a parameter of bias, $\vec{x}_i$ is a feature vector of the input space with dimension D, and y_i is the output value to be estimated.

The SVR uses a more sophisticated penalty function: a penalty is not imposed if the predicted value y_i is less than a distance ε away from the actual value t_i, i.e., if $|t_i - y_i| < \varepsilon$. Referring to Fig. 5, the region bound by $y_i \pm \varepsilon$ for all i is called an ε – insensitive tube. Another modification to the penalty function is that output variables outside the tube are allocated one of two slack variable penalties, depending on whether they lie above (ξ^+) or below (ξ^-) the tube, where $\xi^+ > 0$, $\xi^- > 0$ for all i:

$$t_i \leqslant y_i + \varepsilon + \xi^+, \tag{2}$$

$$t_i \geqslant y_i - \varepsilon - \xi^-. \tag{3}$$

The task is then to find a functional form for f that can correctly predict new cases that the SVM has not been presented with before. This can be achieved by training the SVM model on a sample set called *training set*, a process that involves the

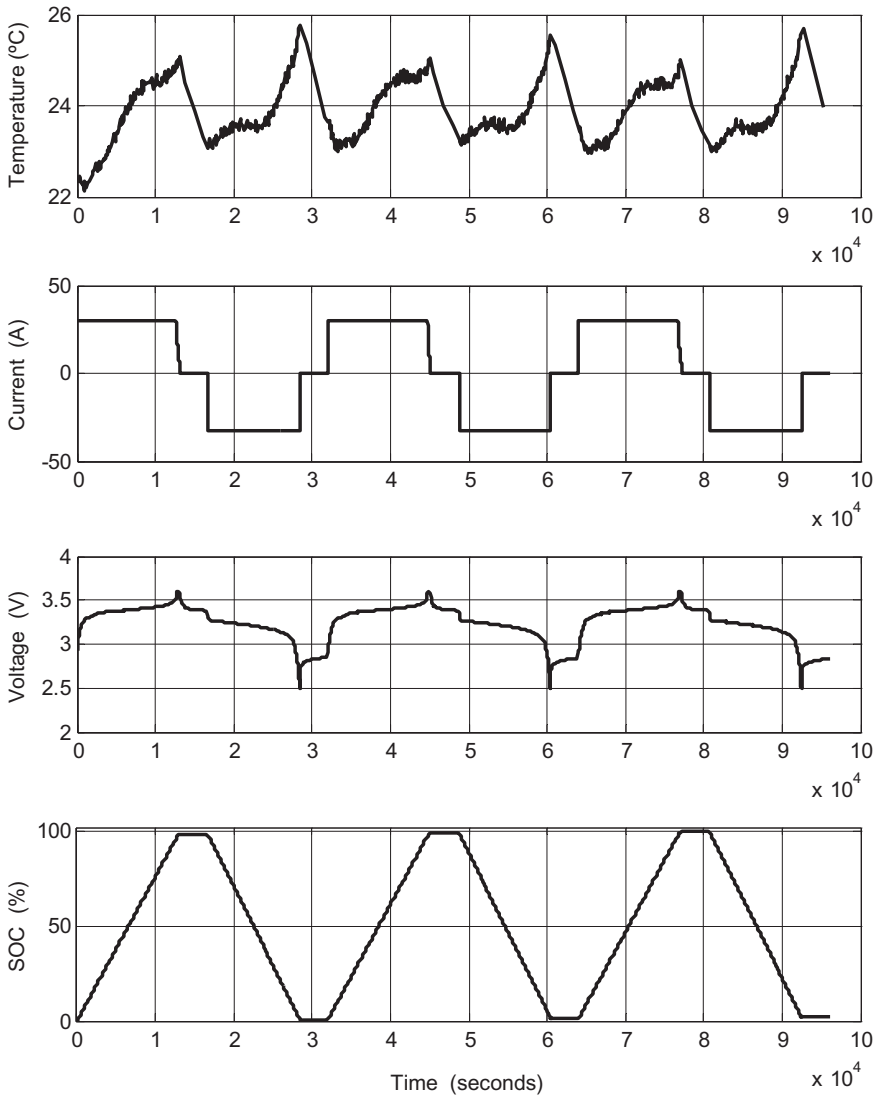

Fig. 3. Training data: cell temperature, current, voltage and SOC vs. time during three charging-discharging cycles. Discharge is performed at C/3 rate (33 A).

sequential optimization of an error function. Depending on the definition of this error function, two types of SVM models can be recognized and the resulting SVM problem [24,19,11] can be formulated as follows:

(a) Regression SVM Type 1 (also known as ε - SVM regression): for this type of SVM, we have to solve an optimization problem minimizing the following general risk function [24,13,11]:

$$R[\vec{w}, b, \xi] = \frac{1}{2}\|\vec{w}\|^2 + C\sum_{i=1}^{L}(\xi_i^+ + \xi_i^-), \tag{4}$$

subject to

$$\left\{\begin{array}{c} \langle \vec{w}, \psi(\vec{x}_i)\rangle + b - y_i \leqslant \varepsilon + \xi_i^+ \\ y_i - \langle \vec{w}, \psi(\vec{x}_i)\rangle - b \leqslant \varepsilon + \xi_i^- \\ \xi_i^+, \xi_i^- \geqslant 0 \end{array}\right\} \quad i = 1, \ldots, L. \tag{5}$$

The first term of Eq. (4) $(1/2\|\vec{w}\|^2)$ is used as a measurement of function flatness. The second term of the general risk function (see Eq. (4)) is the so-called empirical error (risk) measured by the ε - insensitive loss function, which indicates that there are no penalty errors below ε.The ε - insensitive loss function is used to stabilize estimation. In other words, the ε - insensitive loss function can reduce the noise. Finally, the cost function (or regularization constant) C determines the trade-off between the margin (model flatness) and the magnitude of the slack variables (ξ_i^+ and ξ_i^-).

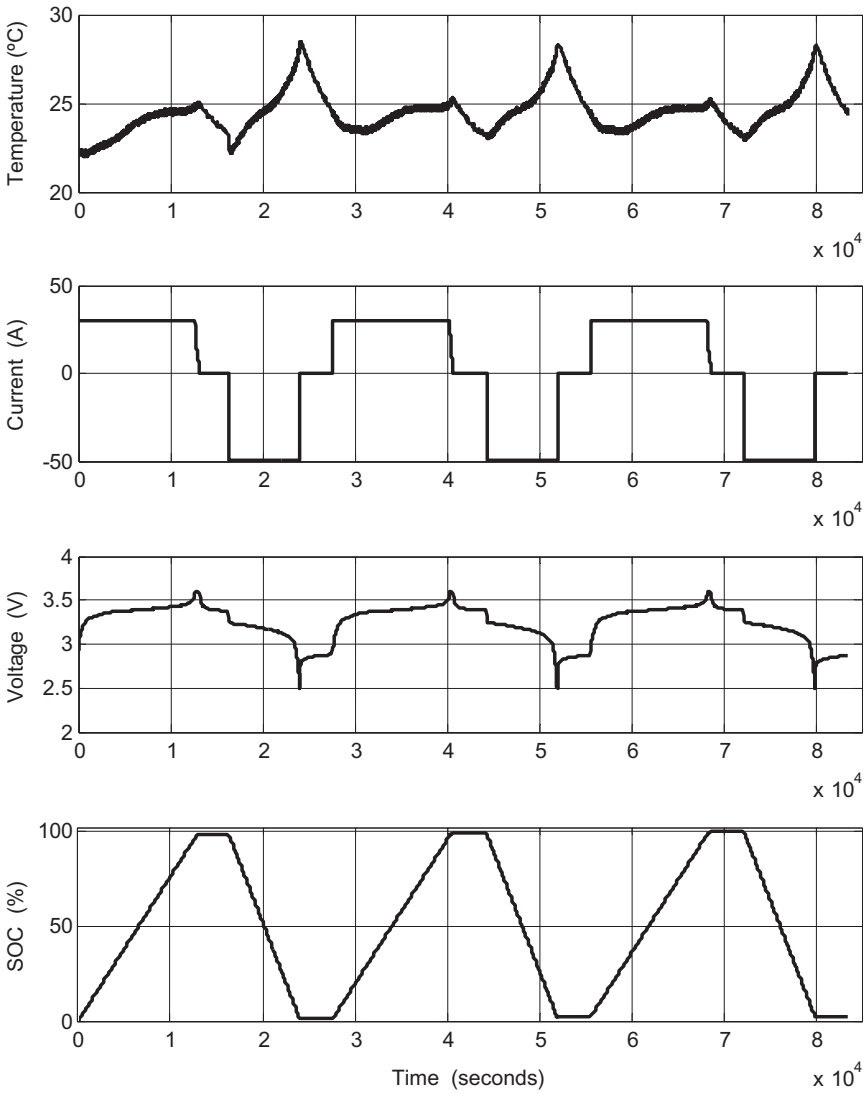

Fig. 4. Validation data: cell temperature, current, voltage and SOC vs. time during three charging-discharging cycles. Discharge is performed at C/2 rate (50 A).

(b) Regression SVM Type 2 (also known as $v-$ SVM regression): for this SVM model, it is necessary to solve the following optimization problem, minimizing the following general risk function [24,13,11]:

$$R[\vec{w},b,\xi]=\frac{1}{2}\|\vec{w}\|^2-C\left[v\varepsilon+\frac{1}{L}\sum_{i=1}^{L}(\xi_i^+ +\xi_i^-)\right], \tag{6}$$

subject to

$$\left\{\begin{array}{c}\langle\vec{w},\psi(\vec{x}_i)\rangle+b-y_i\leqslant\varepsilon+\xi_i^+\\ y_i-\langle\vec{w},\psi(\vec{x}_i)\rangle-b\leqslant\varepsilon+\xi_i^-\\ \xi_i^+,\xi_i^-\geqslant 0\end{array}\right\}\quad i=1,\ldots,L, \tag{7}$$

where v parameter controls the number of support vectors and training errors. To be more precise, v is an upper bound on the fraction of margin errors and a lower bound of the fraction of support vectors.

The function $\psi:X\rightarrow Z$ is a transformation of the input space into a new feature space Z, usually a larger dimension space, where we define an inner product by means of a positive definite function k (kernel trick) [10,14,15]:

$$\langle\psi(\vec{x}),\psi(\vec{x}')\rangle=\sum_i\psi_i(\vec{x})\psi_i(\vec{x}')=k(\vec{x},\vec{x}'). \tag{8}$$

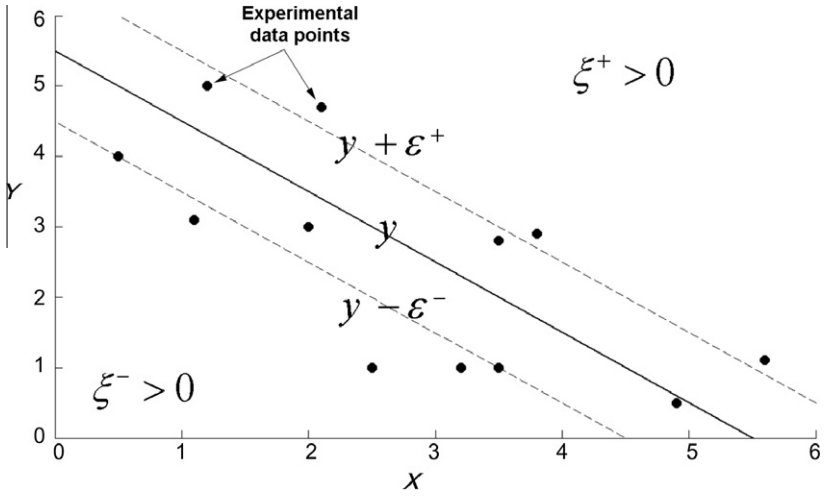

Fig. 5. Regression with ε - insensitive tube.

The above problem is quadratic with linear constraints, and so the Kuhn–Tucker optimality conditions are necessary and sufficient. The solution, which can be obtained from the dual problem, is a linear combination of a subset of sample points denominated support vectors as follows [16,17,19]:

$$\vec{w} = \sum_{s.v.} \beta_i \psi(\vec{x}_i) \Rightarrow \tag{9}$$
$$f_{w,b}(\vec{x}) = \sum_{s.v.} \beta_i \langle \psi(\vec{x}_i), \psi(\vec{x}) \rangle + b = \sum_{s.v.} \beta_i k(\vec{x}_i, \vec{x}) + b.$$

The reason that this kernel trick is useful is that there are many regression problems that cannot be linearly regressed in the space of the inputs $\vec{x}$, which might be in a higher dimensional feature space given a suitable mapping. Different kernel functions are described in the bibliography:

(a) Radial basis function (RBF) [24,11,12]:

$$k(\vec{x}_i, \vec{x}_j) = e^{-\left(\frac{\|\vec{x}_i - \vec{x}_j\|^2}{2\sigma^2}\right)}. \tag{10}$$

(b) Polynomial kernel [24,11,12]:

$$k(\vec{x}_i, \vec{x}_j) = (\vec{x}_i \cdot \vec{x}_j + a)^b, \tag{11}$$

where a and b are parameters defining the kernel's behaviour.

The RBF is by far the most popular choice of kernel types used in support vector machines. This is mainly because of their localized and finite responses across the entire range of the real x-axis. To sum up, to use an SVM to solve a regression problem for data that is not linearly separable, we need to first choose a kernel and relevant parameters that can be expected to map the nonlinearly separable data into a feature space where it is linearly separable. Furthermore, it is well known that the SVM techniques are strongly dependent on the SVM hyperparameters: the regularization factor C (see Eqs. (4) and (6)), the hyperparameter ε that defines the ε - insensitive tube and σ that represents the kernel parameter if a radial basis function (RBF) is chosen. There exists a vast body of literature regarding the choice of hyperparameters for SVMs [11]. Some methods often used to determine suitable hyperparameters are [19,11,25]: cross-validation, random search, grid search, Nelder–Mead search, heuristic search, genetic algorithms, particle swarm optimization, pattern search, etc.

3. Analysis of results and discussion

The cell input variables considered in this study are shown in Table 2. The battery voltage, temperature and current measurements are given as input to the SVM model. The model is trained using the data-set shown in Figs. 2 and 3.

An exhaustive cross-validation algorithm is used to guarantee the predictive ability of the SVM model. In the present study, 10-fold cross-validation is used [25]. Cross-validation is a way to predict the fit of a model to a hypothetical validation set when an explicit validation set is not available. One round of cross-validation involves partition, the data set is randomly divided into l disjoint subsets of equal size, and each subset is used once as a validation set, while the other $l - 1$ subsets are put together to form a training set. In the simplest case, the average accuracy of the l validation sets is used as an estimator for the accuracy of the method. In this way, 10-fold cross-validation was used. The combination of the hyperparameters with

Table 2
Set of battery cell input variables used in this study.

Input variables	Name of the variable
Cell voltage (V)	Voltage
Cell current (A)	Current
Cell temperature (°C)	Temp

Table 3
Optimal hyperparameters of the fitted SVM model.

Parameters	Value
SVM-type	v-regression
SVM-kernel	Radial basis function
γ	0.25
v	0.5
Number of support vectors	12984

the best performance is chosen [13,16,19]. Table 3 shows the optimal hyperparameters of the fitted SVM model used in this research work.

However, it is important to estimate how well a model performs on *new* data. Thus, in order to obtain a robust testing result, an explicit validation data-set is used in this study. The validation data are obtained from running a simple SOC test; see Fig 4. It should be note that the data in Fig. 4 is not used to train the model. The comparison between predicted SOC values using the validation data-set and observed SOC data is shown in Fig. 6. The results clearly show that the fitting is significantly good. The coefficient of determination R^2 was chosen in this research study to estimate the goodness of fit of the SVM model [26]. This ratio indicates the proportion of total variation in the dependent variable explained by the model. A dataset takes values t_i, each of which has an associated modelled value y_i. The former are called the observed values and the latter are often referred to as the predicted values. Variability in the dataset is measured through different sums of squares:

- $SS_{tot} = \sum_{i=1}^{n} (t_i - \bar{t})^2$: the total sum of squares, proportional to the sample variance.
- $SS_{reg} = \sum_{i=1}^{n} (y_i - \bar{t})^2$: the regression sum of squares, also called the explained sum of squares.
- $SS_{err} = \sum_{i=1}^{n} (t_i - y_i)^2$: the residual sum of squares.

In these sums, $\bar{t}$ is the mean of the n observed data:

$$\bar{t} = \frac{1}{n} \sum_{i=1}^{n} t_i. \tag{12}$$

Bearing in mind the above sums, the general definition of the coefficient of determination is

$$R^2 \equiv 1 - \frac{SS_{err}}{SS_{tot}}. \tag{13}$$

A coefficient of determination value of 1.0 indicates that the regression curve fits the data perfectly. In this study, the fitted SVM model has a coefficient of determination equal to 0.97. This result confirms the accuracy of the SOC prediction during charging and discharging using SVM. Moreover, Fig. 6 shows that there is no drift over time in SOC estimation by the SVM model. The SVM model estimates SOC with the largest error when the current is zero at full charge. Small peaks can be seen in the SOC prediction curve at the points that match the input current transient points. Note that the input current is constant except at the step-change points, where current jumps from one steady state value to another. From the mathematical point of view, these peaks correspond to points of discontinuity of the current function and reflect the peculiar manner in which the functions behave at a jump discontinuity: a Gibbs-like phenomenon [27].

It is important to know the implementation requirements of SVM in a practical application. SVM model can make predictions quickly due to the fact that the prediction function simply has to evaluate a manageable number of support vectors. This result means a minimal computation load. For example, SVM usually does not require matrix inversion and intensive calculations which are required by others approaches [3]. The developed model is able to predict the SOC quickly and fairly accurately using the right training data and propel kernel functions [11]. All these features make the SVM model suitable for implementation on a low cost microcontroller-based Battery Management System (BMS) to fulfill the function of the SOC prediction. One of the main tasks of a BMS is to keep track of a battery's SOC. One possible application of accurate SOC information would be for controlling charging. A battery would then always be correctly charged, implying a longer cycle life. Finally, the model can be easily modified to successfully fit data from different batteries, as SVM models are more robust and flexible than linear regression models [19,26].

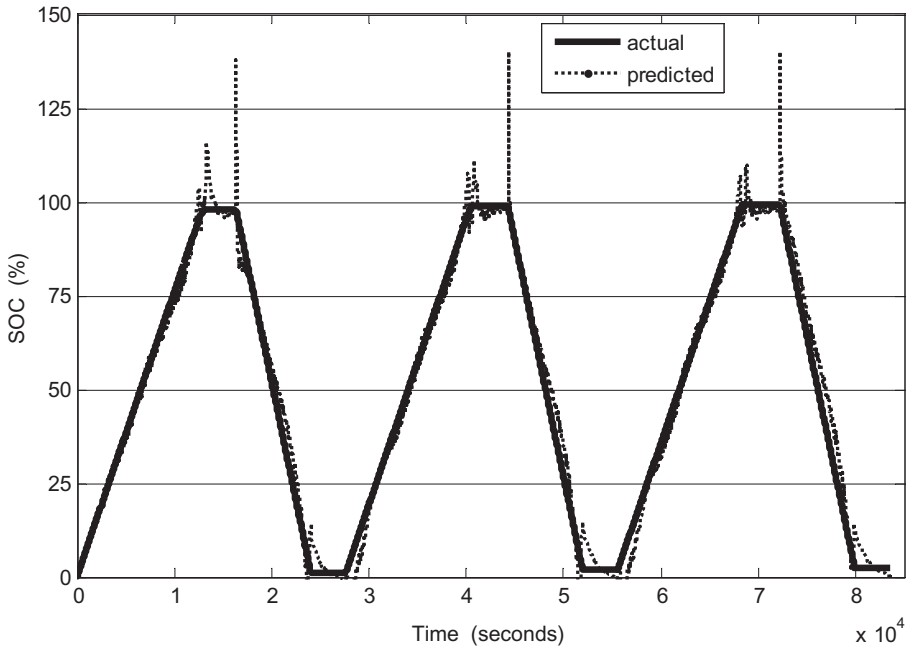

Fig. 6. SOC predicted by SVM vs. actual SOC.

4. Conclusions

To summarize, accurate SOC indication is important for user convenience and for prolonging the lifetime of batteries. However, many examples of poor accuracy and reliability are found in practice. In this sense, there is an absolute necessity in developing alternative prediction techniques such as SVR approach used in this study. The major findings of the study are as follows:

- First, the main purpose of this research work was to build a SOC predictive model using the SVR approach for a high capacity lithium iron phosphate ($LiFePO_4$) battery cell. The proposed SOC estimator extracts model parameters from battery charging/discharging testing cycles, using voltage, current and temperature data as independent variables.
- Second, a coefficient of determination as high as 0.97 is obtained when the SVM model is validated with new data not used for training. The results confirm the accurate predictions of SOC.
- Third, a quick SOC prediction is also obtained, seeing as the prediction function simply has to evaluate the support vectors, which can be manipulated by an inexpensive digital processor. The SVM model may thus be implemented on a low cost microcontroller-based BMS system to fulfill the function of the SOC prediction.
- Finally, the authors of this research work have confidence that the results obtained will be useful to tackle new future studies in other similar battery cells by applying the same methodology.

Acknowledgments

This work was partially supported by the Spanish Science and Innovation Ministry (MICINN), project reference: Plan Nacional, MICINN-10-IPT-370000-2010-15, "Tecnologías de gestión energética para aplicaciones ferroviarias (SIENER)". Authors wish to acknowledge the computational support provided by the Departments of Mathematics, Construction and Mining Exploitation at University of Oviedo.

References

[1] S. Piller, M. Perrin, A. Jossen, Methods for state-of-charge determination and their applications, J. Power Sources 96 (2001) 113–120.
[2] C. Chan, L.E. Lo, S. Weixiang, The available capacity computation model based on artificial neural network for lead-acid batteries in electric vehicles, J. Power Sources 87 (2000) 201–204.
[3] G. Plett, Extended Kalman filtering for battery management systems of LiPB-based HEV battery packs. Part 2. Modeling and identification, J. Power Sources 134 (2004) 262–276.
[4] H. Dai, X. Wei, Z. Sun, Online cell SOC estimation of Li-ion battery packs using a dual time-scale Kalman filtering for EV applications, Appl. Energy (2012), http://dx.doi.org/10.1016/j.apenergy.2012.02.044.

[5] J. Kim, S. Lee, B.H. Cho, Complementary cooperation algorithm based on DEKF combined with pattern recognition for SOC/capacity estimation and SOH prediction, IEEE Trans. Power Electron. 27 (2012) 436–451.
[6] M. Verbrugge, Adaptive, multi-parameter based state estimator with optimized time-weighting factors, J. Appl. Electrochem. 37 (2007) 605–616.
[7] Y. Hu, S. Yurkovich, Battery cell state-of-charge estimation using linear parameter varying system techniques, J. Power Sources (2011), http://dx.doi.org/10.1016/ j.jpowsour.2011.09.05, 2011.
[8] I. Kim, Nonlinear state of charge estimator for hybrid electric vehicle battery, IEEE Trans. Power Electron. 23 (2008) 2027–2034.
[9] J. Kim, J. Shin, C. Chun, B.H. Cho, Stable configuration of a Li-ion series battery pack based on a screening process for improved voltage/SOC balancing, IEEE Trans. Power Electron. 27 (2012) 411–424.
[10] V. Vapnik, Statistical Learning Theory, Wiley-Interscience, 1998.
[11] I. Steinwart, A. Christmann, Support Vector Machines, Springer, 2008.
[12] T. Hastie, R. Tibshirani, J.H. Friedman, The Elements of Statistical Learning, Springer, 2009.
[13] B. Schölkopf, A.J. Smola, Learning with Kernels: Support Vector, Machines Regularization, Optimization and Beyond, The MIT Press, 2002.
[14] T.S. Furey, N. Cristianini, N. Duffy, D.W. Bednarski, M. Schummer, D. Haussler, Support vector machine classification and validation of cancer tissue samples using microarray expression data, Bioinformatics 16 (2000) 906–914.
[15] G. Guo, S.Z. Li, K.L. Chan, Support vector machines for face recognition, Image Vision Comput. 19 (2001) 631–638.
[16] J. Taboada, J.M. Matías, C. Ordóñez, P.J. García Nieto, Creating a quality map of a slate deposit using support vector machines, J. Comput. Appl. Math. 204 (2007) 84–94.
[17] X. Li, D. Lord, Y. Zhang, Y. Xie, Predicting motor vehicle crashes using support vector machine models, Accid. Anal. Prev. 40 (2008) 1611–1618.
[18] S. Haykin, Neural Networks, A comprehensive foundation, Prentice Hall, 1999.
[19] J. Shawe-Taylor, N. Cristianini, Kernel Methods for Pattern Analysis, Cambridge University Press, 2004.
[20] T. Hansen, C.J. Wang, Support vector based battery state of charge estimator, J. Power Sources 141 (2005) 351–358.
[21] J. Essick, Hands-on Introduction to LabVIEW for Scientists and Engineers, Oxford University Press, 2009.
[22] J.C. Viera, M. Gonzalez, B.Y. Liaw, F.J. Ferrero, J.C. Alvarez Anton, J.C. Campo, C. Blanco, Characterization of 109 Ah NiMH batteries charging with hydrogen sensing termination, J. Power Sources 171 (2007) 1040–1045.
[23] C. Carballo, M. Gonzalez, J.C. Alvarez Antón, C. Blanco, A computerized system for testing batteries in full controlled environment, Proc. IEEE Instrum. Meas. Technol. Conf. 1 (2000) 395–399.
[24] T. Fletcher, Support Vector Machines Explained: Introductory Course, University College London (UCL), Internal Report, 2009.
[25] R. Picard, D. Cook, Cross-validation of regression models, J. Am. Stat. Assoc. 79 (1984) 575–583.
[26] L. Wasserman, All of Statistics: A Concise Course in Statistical Inference, Springer, 2003.
[27] A.J. Jerri, Advances in the Gibbs Phenomenon, Sampling Publishing, 2011.